EuroIntervention 2012;8:708-716

Plaque distribution patterns in left main trunk bifurcations: prediction of branch vessel compromise by multidetector row computed topography after percutaneous coronary intervention

Yoshitaka Goto, MD; Tomohiro Kawasaki*, MD; Nobuhiko Koga, MD; Hidenori Tanaka, MD; Hisashi Koga, MD; Yoshiya Orita, MD; Shinsuke Ikeda, MD; Yoshiaki Shintani, MD; Masataka Kajiwara, MD; Takaya Fukuyama, MD

Department of Cardiology, Cardiovascular Center, Shin-Koga Hospital, Kurume, Japan

KEYWORDS

- percutaneous coronary interventions
- bifurcation lesions
- cardiac computed tomography
- carina shift
- left main trunk

Abstract

Aims: We investigated the mechanism and predictors of jailed branch vessel (BV) compromise during the stenting of left main trunk (LMT) bifurcation lesions from a multidetector row computed tomography (MDCT) analysis.

Methods and results: Eighty patients who underwent MDCT and stenting for LMT bifurcation lesions were examined. The patients were retrospectively classified into a BV stenosis (BVS; n=38) group and a non-BV stenosis (NBVS; n=42) group according to a coronary angiography obtained just after crossover stent deployment for the target vessel (TV). The angle between the LMT and TV was significantly wider in the BVS group than in the NBVS group (140.2±10.3 degree vs. 132.6±14.2 degree, p=0.0076), and the frequency of carina side plaque at the TV in the long and short axis was significantly higher in the BVS group than in the NBVS group (50.0% vs. 16.7%; p=0.0012, 63.2% vs. 38.1%; p=0.0251, respectively). In a multivariate analysis, the presence of carina side plaque at the TV in the long and short axis were independent predictors of BVS (odds ratio: 5.15, p=0.0086, odds ratio: 3.83, p=0.0231, respectively).

Conclusions: The plaque distribution and morphology assessed by MDCT may provide useful information that can predict the potential compromise of the BV during treatment for an LMT bifurcation lesion.

Corresponding author: Department of Cardiology, Cardiovascular Center, Shin-Koga Hospital, 120, Tenjin-cho, Kurume, 830-8577 Japan. E-mail: to-kawasaki@mug.biglobe.ne.jp

DOI: 10.4244/EIJV8I6A110

Abbreviations

PCI	percutaneous coronary intervention
DES	drug-eluting stent
LMT	left main trunk
CABG	coronary artery bypass graft
BV	branch vessel
IVUS	intravascular ultrasound
CT	computed tomography
TV	target vessel
LAD	left anterior descending coronary artery
LCX	left circumflex coronary artery
BVS	branch vessel stenosis
NBVS	non-branch vessel stenosis
QCA	quantitative coronary angiography
3D-VR	three-dimensional volume rendering
RI	remodelling index
CCP	colour code plaque
OR	odds ratio
CI	confidence interval

Introduction

Percutaneous coronary interventions (PCI) for bifurcation lesions comprise 15~20% of all PCI procedures in daily practice, and are associated with a relatively high restenosis rate as well as a high incidence of procedural complications including side branch occlusion and myocardial infarction[1,2]. PCI for bifurcations are thus still a challenging treatment, even in the drug-eluting stent (DES) era. This is particularly true in the case of left main trunk (LMT) bifurcation lesions where current guidelines consider coronary artery bypass grafting (CABG) as the "gold standard"[3,4], and where major branch vessel (BV) compromise can occur, perhaps leading to a critical situation. Therefore, being able to predict whether a major BV compromise will occur is an important issue for the successful treatment of LMT bifurcation lesions.

Assessments regarding possible predictors of BV compromise by coronary angiography[1,5] and intravascular ultrasound (IVUS)[6] have been reported. In particular, IVUS provides precise information about the plaque with high quality images. However, IVUS is invasive and may provide warped geometric information due to its inherent limitations. On the other hand, although it does result in radiation exposure, cardiac multidetector row computed tomography (MDCT) is a less invasive tool for assessing the coronary anatomy, including plaque distribution, and is known to have excellent detectability of the plaque, similar to IVUS[7,8].

The recent consensus regarding jailed BV compromise is that it is now thought to be a carina shift rather than plaque shift[9,10]. However, no previous investigation about the correlation between the carina shift and the bifurcation anatomy, including the plaque distribution, has been reported.

In the present study, we investigated the mechanism involved – and the predictors of – jailed BV compromise during the stenting of LMT bifurcation lesions from a cardiac CT analysis.

Methods

PATIENT POPULATION AND THE PCI PROCEDURE

One hundred and twelve consecutive patients who underwent cardiac CT and then underwent PCI for a LMT bifurcation lesion within 30 days between January 1, 2006 and April 30, 2010 in our cardiovascular centre were included in this study. All lesions were *de novo* and had significant stenosis of more than 50% of the diameter. All patients underwent stent implantation from the LMT to the target vessel (TV) across the BV without predilation of the BV. If the left anterior descending coronary artery (LAD) was the TV, then the left circumflex coronary artery (LCX) was defined as the BV, and vice versa. The patients who had undergone CABG or had heavy calcified LMT bifurcation lesions, which confounded the CT evaluations, were excluded from the analysis. Heavy calcification was defined as circumferential (over 180 degrees) calcification measuring over 5 mm in length. Finally, 80 patients with 80 LMT bifurcation lesions were investigated in this study **(Figure 1)**.

The patients were retrospectively classified into two groups according to their coronary angiography results obtained just after the first stent implantation: a BV stenosis (BVS) group and a non-BV stenosis (NBVS) group. BVS was defined as the progression of more than 75% diameter stenosis or two stage progression of the American Heart Association classification[11] (e.g., from 0% to 50%, and from 25% to 75%) of the BV ostium as determined by the quantitative coronary angiography (QCA) analysis. QCA was performed using the semi-automatic edge contour-detection computer analysis system, Centricity Cardiology AI 1000 version 4.1.15 (GE Healthcare, Milwaukee, WI, USA). The QCA analysis was performed by more than two cardiovascular physicians who were blinded to the study results. In cases of disagreement, the opinion was made by consensus.

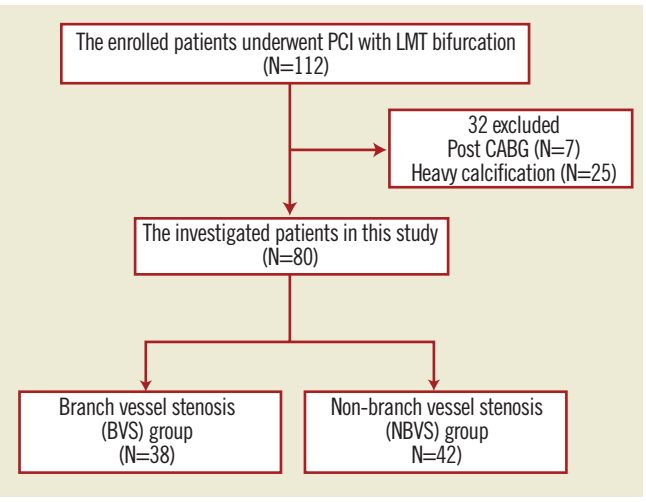

Figure 1. *The study flow chart. Of 112 consecutive patients, 80 patients with 80 LMT bifurcation lesions were investigated. PCI: percutaneous coronary intervention; LMT: left main trunk; CABG: coronary artery bypass graft*

The PCI strategy and the device selection (guidewire, balloon, stent type, etc.) were left to the operator's discretion. All patients were fully informed about the possible procedure-related risks and the alternative treatment options, and written informed consent was obtained in all cases.

CT ANGIOGRAPHY: IMAGE ACQUISITION

Almost all of the enrolled patients received oral and/or intravenous beta-blockers to achieve a heart rate of <65 beats/min and were given one puff of nitroglycerine spray just before the examination if it was not contraindicated. CT angiography (CTA) was obtained by a 64 row-CT scanner (Lightspeed VCT, GE Healthcare, Milwaukee, WI, USA) using a double phase contrast protocol: 40 to 60 ml iodine (Iopamiron; Bayer Health Care, Osaka, Japan), followed by a 20 ml flush with a 50:50 mixture of iodine and saline. Before the main scan, a test injection was performed to determine the delay time, and a monitoring scan was acquired at the centre of the ascending aorta. A measurement curve was created during the test injection. The scan parameters included 64×0.625 mm collimation, tube voltage 120 kV, 350 to 800 mA, the gantry rotation speed was 350ms/rotation and dose-modulated retrospective electrocardiogram-gating was used. If the heart rate was <60 beats/min, a prospective electrocardiogram-gating scan was used.

CT ANGIOGRAPHY: DATA ANALYSIS

Each coronary bifurcation angle, between the LMT and the TV (∠LMT-TV), between the LMT and the BV (∠LMT-BV) and between the TV and the BV (∠TV-BV), was measured by using the three-dimensional volume rendering (3D-VR) coronary tree image. The standard axial images, and oblique long- and short-axis multiplanar reconstruction were used to classify lesions having significant stenosis, which was defined as a diameter reduction by >50%. The type of bifurcation lesion was assessed by the Medina classification[12], and Medina (1, 1, 1) and (0, 1, 1) were defined as true bifurcation lesions.

The reference vessel areas of the LMT, TV and BV were measured as the average of the vessel area at both the proximal and distal sites. The lesion vessel area and lesion lumen area were measured at the lesion site with maximal lumen narrowing on cross-sectional images.

The vessel area was defined as the enclosed area with the outer vessel line. The percent plaque area was calculated as (1– lumen area/vessel area) ×100. The arterial remodelling index (RI) was also assessed and was calculated by the vessel area at the lesion site with maximal lumen narrowing divided by the reference vessel area for each vessel. The vessel area ratio was defined as the ratio of the reference vessel area between the LMT and the MV or the BV, and was calculated by the reference vessel area of the MV or the BV divided by that of the LMT.

The plaque volume and plaque consistency were assessed automatically by Colour Code Plaque™ (CCP) analysis (GE Healthcare)[13,14]. The CCP analysis was based on the stratified CT density within 5 mm proximal in the LMT and distal in the MV from the carina. The plaque consistency was classified into two categories, <50 HU as a low attenuation plaque and 50 HU to 150 HU as an intermediate attenuation plaque.

The plaque distribution around the LMT bifurcation area was assessed for the long and short axes **(Figure 2)**. In the long axis view, bifurcation lines were defined as the extended line from the carina (black dotted lines) and the plaque position was classified into six parts: "A" and "B" were the outer side of the LMT-TV; "C" was the carina side of the TV; "D" was the carina side of the BV; and "E" and "F" were the outer side of the LMT-BV **(Figure 2A)**. In the short axis view, the plaque position was assessed 1 mm distal from the bifurcation line (red dotted lines) and was classified into eight parts: "a" and "h" were the outer wall side; "b" and "g" were the myocardial side; "c" and "f" were the pericardial side; and "d" and "e" were the carina side in the MV and in the BV, respectively **(Figure 2B)**. Regarding the short axis division, we referred to the previous study published by van der Giessen et al[15]. We next checked the plaque distribution and counted the number of plaques located in both the long and short axes in all lesions.

All data were analysed using the Advantage Workstation software programme, version 4.4 (GE Healthcare, Milwaukee, WI, USA) by two cardiovascular physicians who were blinded to the study results. In case of disagreement, the opinion was made by consensus.

STATISTICAL ANALYSIS

Continuous data were summarised as the means ±SD. Categorical data were summarised as counts and percentages. Unpaired t-tests were used for comparing the continuous variables, and the chi squared test and Fisher's exact test were used for categorical variables. A multivariate analysis was used to examine independent risk factors related to the progression of the BV stenosis. A value of

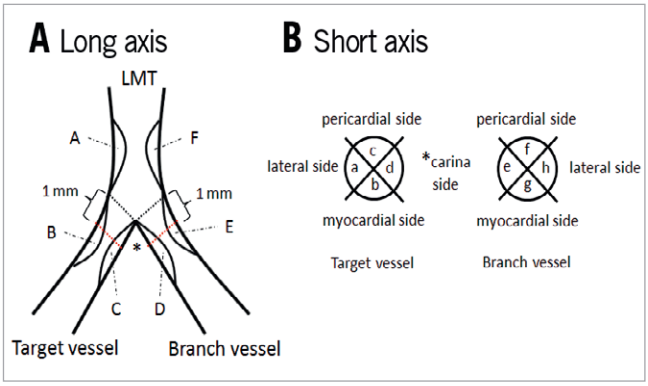

Figure 2. *The description of plaque distribution at the LMT bifurcation area. The bifurcation lines were defined as the extended line from the carina (black dotted lines). A) The long axis view. The plaque position was classified into categories from 'A' to 'F'. B) The short axis view. The plaque position was classified into categories from 'a' to 'h' at 1 mm distal from the bifurcation lines (red dotted lines). LMT: left main trunk*

p<0.05 was considered to be statistically significant. All statistical analyses were performed with the JMP statistical software programme version 9.0.2 (SAS Institute Japan, Tokyo, Japan).

Results

The study flow chart is shown in **Figure 1**. Finally, a total of 80 patients (51 males, mean age 68.7±10.3 years) with 80 LMT bifurcation lesions were investigated, and 38 patients (47.5%) were assigned to the BVS group and 42 (52.5%) were assigned to the NBVS group. Their baseline characteristics are listed in **Table 1**. There were no significant differences in these characteristics between the two groups.

The lesion characteristics, procedural information and data from CT are summarised in **Table 2**. Regarding the bifurcation information, there was no significant difference in the true bifurcation rate between the BVS group and NBVS group (23.7% vs. 14.3%; p=0.2880), whereas the ∠LMT-TV was significantly wider in the BVS group than in the NBVS group (140.2±10.3 degree vs. 132.6±14.2 degree, p=0.0076). The bifurcation plaque components evaluated by CCP analysis were similar in their proportion between the two groups, and about 70% of the plaque components were fibro-calcified over 50 HU in both groups. The correlation between the plaque distribution and the frequency around the LMT bifurcation is shown in **Figure 3**. The frequency of the "C" in the long axis and the "d" in the short axis were significantly higher in the BVS group compared with the NBVS group (50.0% vs. 16.7%; p=0.0012, 63.2% vs. 38.1%; p= 0.0251, respectively).

In the multivariate analysis, the plaque deposit at "C" in the long axis and that at "d" in the short axis were identified as the independent predictive factors which might influence the BVS (odds ratio [OR]: 5.147, 95% confidence interval [CI]: 1.585 - 18.80, p=0.0086, OR: 3.832, 95% CI: 1.246-13.00, p=0.0231, respectively) **(Table 3)**.

Representative cases are shown in **Figure 4** and **Figure 5**.

Table 1. The baseline characteristics of the study population.

	All (n=80)	BVS group (n=38)	NBVS group (n=42)	*p*-value
Age, yrs	68.7±10.3	70.1±10.4	67.5±10.1	0.2736
Male	51 (63.8%)	22 (57.9%)	29 (69.0%)	0.3061
BMI, kg/m^2	23.6±3.1	23.0±3.2	24.1±3.0	0.1106
Hypertension	66 (82.5%)	31 (81.6%)	35 (83.3%)	0.8391
Current smoking	12 (15.0%)	6 (15.8%)	6 (14.3%)	0.8531
Diabetes mellitus	35 (43.8%)	15 (39.5%)	20 (47.6%)	0.4696
Dyslipidaemia	66 (82.5%)	31 (81.6%)	35 (83.3%)	0.8391
CKD	10 (12.5%)	5 (13.6)	5 (11.9%)	0.8677
ACS	15 (18.8%)	10 (26.3%)	5 (11.9%)	0.1016
Prior PCI history	28 (35.0%)	13 (34.2%)	15 (35.7%)	0.8898

The values are shown as the mean±SD or n (%). BVS: branch vessel stenosis; NBVS: non branch vessel stenosis; BMI: body mass index; CKD: chronic kidney disease; ACS: acute coronary syndrome; PCI: percutaneous coronary intervention

Table 2. The lesion and procedural characteristics and CT findings.

	All (n=80)	BVS group (n=38)	NBVS group (n=42)	*p*-value
Bifurcation angle, degree				
∠LMT-TV	136.2±13.0	140.2±10.3	132.6±14.2	0.0076
∠LMT-BV	128.0±15.8	127.7±18.3	128.2±13.3	0.9008
∠TV-BV	77.4±16.1	75.4±17.2	79.2±15.0	0.2886
Vessel area, mm^2				
LMT	22.8±5.5	22.6±5.0	23.1±5.9	0.6629
TV	17.5±4.8	17.1±4.2	17.9±5.2	0.4430
BV	14.8±4.0	14.7±4.5	15.0±3.5	0.7818
MLA, mm^2				
LMT	10.8±5.1	9.9±4.23	11.6±5.7	0.1253
TV	3.6±2.4	3.7±2.6	3.5±2.1	0.7892
BV	8.4±3.5	8.0±3.5	8.7±3.5	0.3706
% plaque area, %				
LMT	52.2±21.2	55.5±17.9	49.1±23.6	0.1829
TV	78.2±14.9	77.0±16.8	79.2±13.2	0.5165
BV	42.1±21.4	42.5±23.4	41.7±19.6	0.8676
Vessel area ratio				
TV / LMT	0.79±0.21	0.77±0.19	0.80±0.24	0.6104
BV / LMT	0.67±0.19	0.66±0.21	0.67±0.19	0.7903
BV / TV	0.89±0.30	0.90±0.32	0.89±0.29	0.9256
Remodelling index				
LMT	1.05±0.19	1.04±0.23	1.06±0.15	0.7079
TV	1.31±0.23	1.29±0.19	1.33±0.26	0.4878
BV	1.24±0.28	1.28±0.35	1.20±0.21	0.1956
Plaque proportion by CCP analysis, %				
HU <50	29.7±7.0	29.7±6.9	29.7±7.9	0.9936
50 HU <120	40.1±4.8	42.0±4.9	39.1±4.9	0.8379
500 <HU	29.9±12.2	28.3±11.1	31.2±13.3	0.8527

The values are shown as the mean ±SD or n (%). CT: computed tomography; LMT: left main trunk; TV: target vessel; BV: branch vessel; MLA: minimum lumen area; RI: remodelling index; BVS: branch vessel stenosis; NBVS: non branch vessel stenosis

Table 3. Multivariate analysis: predictors of the branch vessel compromise.

	Odds ratio	95% CI	*p*-value
∠LMT-TV	0.96	–0.0932-0.0049	0.0926
∠LMT-BV	1.02	–0.0277-0.0708	0.4158
∠TV-BV	1.03	–0.0132-0.0083	0.1760
TV / LMT ratio	27.0	–4.530-11.432	0.8298
BV / LMT ratio	0.34	–9.8225-7.7501	0.4099
BV / TV ratio	0.95	–6.3048-5.7184	0.8039
"C" in the long axis	5.15	1.585-18.80	0.0086
"d" in the short axis	3.83	1.246-13.00	0.0231

CI: confidence interval; CT: computed tomography; LMT: left main trunk; TV: target vessel; BV: branch vessel

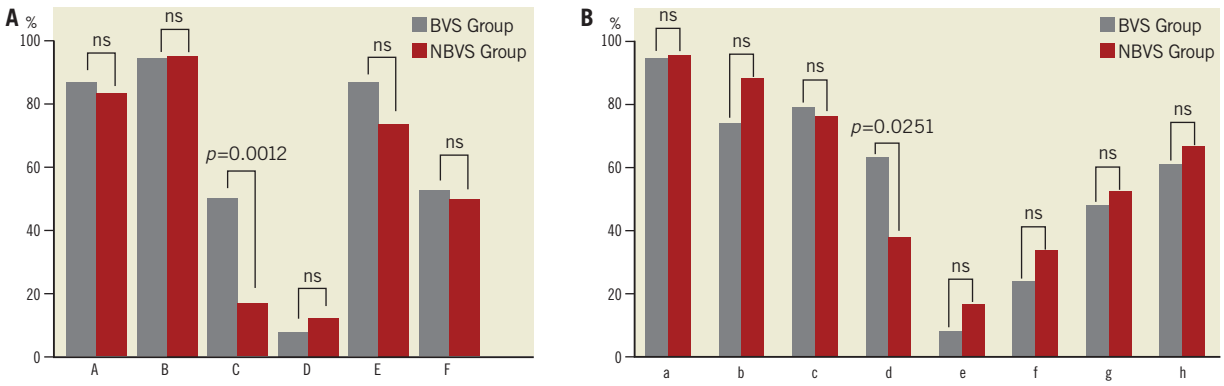

Figure 3. *The plaque distribution pattern at the LMT bifurcation area in the long axis and short axis views. A) The long axis view pattern. B) The short axis view pattern. The frequency of the "C" in the long axis view and the "d" in the short axis view were significantly higher in the BVS group compared with the NBVS group (50.0% vs. 16.7%; p=0.0012, 63.2% vs. 38.1%; p=0.0251, respectively). BVS: branch vessel stenosis; NBVS: non-branch vessel stenosis; LMT: left main trunk*

Discussion

Current guidelines recommend surgical intervention as the "gold standard" for the treatment of unprotected LMT lesions[3,4]. However, since DES has become common in the clinical field, DES has been used aggressively, even in the LMT bifurcation lesions, and the single-stent strategy across the BV is now fundamentally recommended by general consensus[16-20]. In addition, several recent studies have shown both mid- and long-term safety and efficacy of DES for LMT lesions[21-24]. However, about 60% of all bifurcation cases demonstrate disease involvement in the BV ostium[25], and BV compromise can occur under such conditions. In particular, the BV compromise may become a serious situation for LMT bifurcation lesions, and therefore, the prediction of whether BV compromise will occur is important.

Previous studies using either IVUS[6] or invasive angiography[1,5,26] have shown the plaque distribution to have an important effect on BV compromise during bifurcation treatment. Recent remarkable developments in CT technology have now made it possible to noninvasively obtain detailed information on the coronary bifurcation anatomy, including the plaque distribution and the plaque properties, with excellent diagnostic accuracy.

To the best of our knowledge, this is the first clinical study to examine the mechanism and incidence of BV compromise after stenting during the treatment of LMT bifurcation lesions by the use of cardiac CT. The major findings of the present study are that the plaque distribution at the carina side in the TV wall is a predictor of BV compromise during stenting in the LMT bifurcation lesions, and that these plaque components are disclosed as fibrous plaques over 50 HU in the CCP analysis **(Figure 4)**.

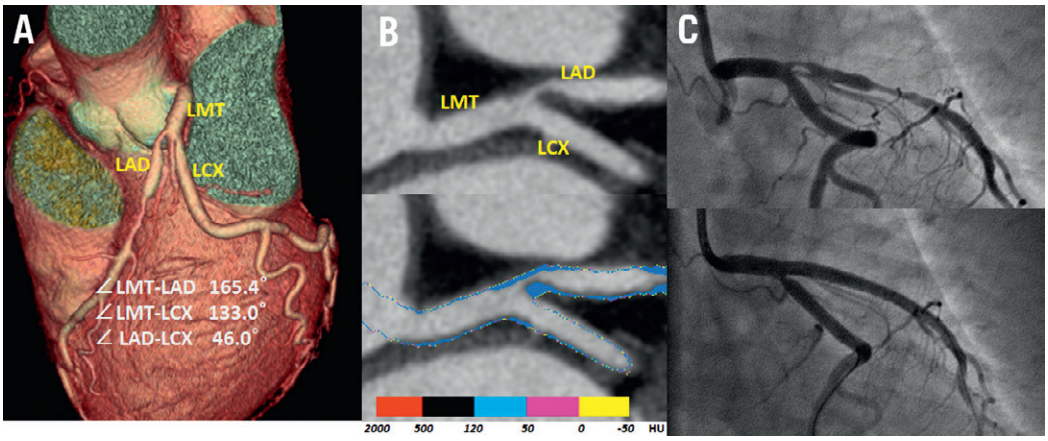

Figure 4. *A representative case with carina shift. The cardiac CT images showed a severe stenosis in the ostial LAD (A) three-dimensional volume rendering image. B) Curved multiplanar reconstruction image clearly showed the plaque at the carina in the target vessel (upper), and the plaque components were depicted as fibrous plaque of more than 50 HU by the colour code plaque analysis image (lower). C) Coronary angiography before stenting (upper) and just after stenting (lower); the ostial LCX was compromised just after LMT stenting. LMT: left main trunk; CT: computed tomography; LAD: left anterior descending artery; LCX: left circumflex coronary artery; HU: Hounsfield unit*

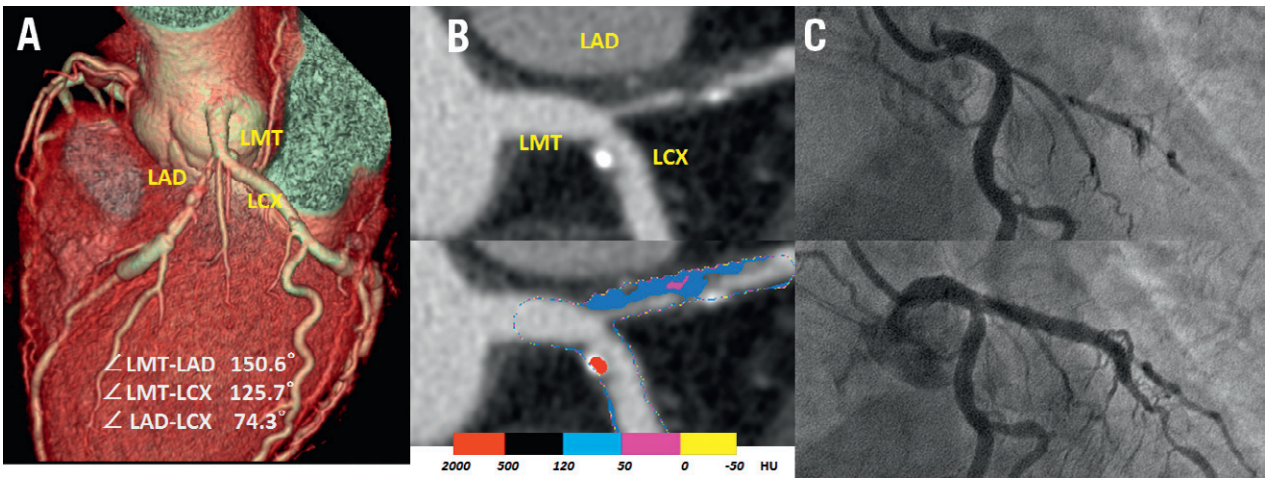

Figure 5. *A representative case without carina shift. The cardiac CT images showed a severe stenosis in the ostial LAD. A) Volume rendering 3-D image. B) Curved multiplanar reconstruction image showed the plaque at the opposite site of carina in the target vessel (upper), the colour code plaque analysis image (lower). C) Coronary angiography before stenting (upper) and just after stenting (lower); the ostial LCX was not compromised after LMT stenting. LMT: left main trunk; CT: computed tomography; LAD: left anterior descending artery; LCX: left circumflex coronary artery; HU: Hounsfield unit*

PLAQUE DISTRIBUTION ASSESSED BY CARDIAC CT

IVUS examination is well known as one of the best modalities to assess intracoronary plaques[27-31]. However, the IVUS catheter and guidewire bias affect the bifurcation geometry and cardiac pulsation also affects the IVUS image. In contrast, CTA noninvasively provides precise 3-D information about the coronary bifurcation angle and the plaque distribution pattern. In addition, regarding the morphological analysis of the plaque, it has been reported that CTA has a high concordance to IVUS measurements[7,8].

Although previous IVUS studies reported that no plaque was documented in the area of the carina[32,33], a recent bifurcation study assessed by CT revealed the plaque distribution in the coronary bifurcation and demonstrated that plaque was observed in the area of the carina accompanied by plaques in the adjacent outer lateral wall[15]. A more recent IVUS study also demonstrated plaque distribution at the carina in approximately 30% of the bifurcations[34]. These observations correspond to the theory that atherosclerotic plaque "grows" from the circumferential wall where there is thought to be a lower shear stress in a bifurcation[15,35,36]. In the present study, the plaque distribution in the LMT bifurcation was clearly demonstrated by CT examination, and the plaque distribution was more frequently observed in the outer lateral wall side than at the carina wall side, according to the grade of shear stress, similar to the previous CT study[15]. It is worth noting that the distribution of the plaque in a lateral wall side was frequently observed both in the BVS group and in the NBVS group, but it did not affect whether the BV would be compromised. In contrast, in the carina side, plaque distribution was infrequently observed in both groups, but a significant difference in the occurrence of BV compromise was observed between the two groups.

MECHANISMS BEHIND A CARINA SHIFT

The recent concept regarding the BV compromise after TV stenting refers to a "carina shift" rather than a "plaque shift"[9,10,37]. This theory is based on a recent study where patients were assessed by IVUS, which reported that no plaque was found in most patients at the level of the carina[33]. However, a more recent study using CTA and IVUS disclosed the presence of plaque in 30% of bifurcations requiring intervention[15,34], which was similar to our present results.

Interestingly, the components of all plaques observed on the carina side in both groups were depicted, not as soft attenuation plaques (<50 HU), but as intermediate attenuation plaques (>50 HU) by the CCP analysis in our present study **(Figure 4)**. This would coincide with the theory that plaques grown into the carina are observed in more advanced atherosclerotic stages[15]. According to recent consensus, the main mechanism involved in BV compromise after stenting is carina shift[9,10,37]. The facts disclosed by our study also support the theory of carina shift. Namely, that intermediate plaques may exert a "mass-effect" toward the BV during TV stenting in bifurcation lesions, which thereby contribute to BV compromise after TV stenting.

On the other hand, neither the bifurcation angle nor the selected stent diameter had any effect on the BV compromise in our study. These two factors are thought to be powerful predictors of side branch compromise after main branch stenting. Vassilev et al showed that the bifurcation angle between the LMT and the BV was an important factor involved in BV compromise from an angiographic analysis[38]. However, it is well known that the 3D-VR on CT can provide more accurate information about the coronary bifurcation angle[39,40] than conventional coronary angiography. In short, the differences in the imaging modality might have affected our results.

Regarding the stent diameter used to treat bifurcation lesions, it is recommended that a stent diameter should be selected according to Murray's law to decrease the risk of BV compromise[41,42]. In this study, we measured each vessel diameter by cross-sectional imaging on CT and found that there were no significant differences between the two groups.

Study limitations

The present study has several limitations. First, this study was a single-centre retrospective study which thus had a relatively small study population.

Second, we examined the mechanisms of BV compromise during TV stenting based on the findings of CT examinations in the present study. Therefore, we measured the vessel size from the cross-sectional image and evaluated the plaque volume and morphology based on the CCP analysis. However, the limitations in the spatial resolution or partial volume effect caused by the contrast media may obscure the border of the vessel wall and, therefore, measuring the exact vessel size and evaluating the plaque characteristics from the CT image remains a difficult challenge. In addition, since IVUS was not routinely performed for all vessels, we could not compare the IVUS images with the CT images.

Third, in the present study, the second CT scan immediately after PCI was not taken to confirm whether carina shift had taken place. It is difficult to assess carina shift using MDCT because it is necessary to dilate the stent struts with simultaneous balloon dilation if the BV were to compromise after stenting. Additionally, the spatial resolution of MDCT is not adequate to complete a detailed evaluation of plaques distribution after stenting. Excessive radiation exposure due to repeated CT scanning also cannot be ignored.

Finally, this study was only focused on LMT bifurcation lesions. Therefore, whether the results of our study can be applied to other bifurcation lesions remains unclear.

Conclusion

The present study demonstrated that plaque distribution and plaque morphology assessed by CT may provide useful information for the operators, and can predict the potential compromise of the BV during treatment for an LMT bifurcation lesion. A larger study population and better resolution CT should be included in a future study to obtain a more exact prediction of BV compromise due to carina shift, and for a more exact evaluation of the plaque morphology during the treatment of LMT bifurcation lesions.

Acknowledgements

The authors thank Miss Mayumi Tsujisho and the other staff members of the cardiac CT unit at our hospital for their technical support for CT scanning and image reconstruction, and Yoshinobu Murasato, MD, for his valuable advice.

Conflict of interest statement

The authors have no conflicts of interest to declare.

References

1. Meier B, Gruentzig AR, King SB 3rd, Douglas JS Jr, Hollman J, Ischinger T, Aueron F, Galan K. Risk of side branch occlusion during coronary angioplasty. *Am J Cardiol.* 1984;53:10-14.

2. Yamashita T, Nishida T, Adamian MG, Briguori C, Vaghetti M, Corvaja N, Albiero R, Finci L, Di Mario C, Tobis JM, Colombo A. Bifurcation lesions: two stents versus one stent--immediate and follow-up results. *J Am Coll Cardiol.* 2000;35:1145-51.

3. Kushner FG, Hand M, Smith SC Jr, King SB 3rd, Anderson JL, Antman EM, Bailey SR, Bates ER, Blankenship JC, Casey DE, Jr, Green LA, Hochman JS, Jacobs AK, Krumholz HM, Morrison DA, Ornato JP, Pearle DL, Peterson ED, Sloan MA, Whitlow PL, Williams DO. 2009 focused updates: ACC/AHA guidelines for the management of patients with ST-elevation myocardial infarction (updating the 2004 guideline and 2007 focused update) and ACC/AHA/SCAI guidelines on percutaneous coronary intervention (updating the 2005 guideline and 2007 focused update) a report of the American College of Cardiology Foundation/American Heart Association Task Force on Practice Guidelines. *J Am Coll Cardiol*. 2009;54:2205-41.

4. Silber S, Albertsson P, Aviles FF, Camici PG, Colombo A, Hamm C, Jorgensen E, Marco J, Nordrehaug JE, Ruzyllo W, Urban P, Stone GW, Wijns W. Guidelines for percutaneous coronary interventions. The Task Force for Percutaneous Coronary Interventions of the European Society of Cardiology. *Eur Heart J*. 2005;26:804-47.

5. Boxt LM, Meyerovitz MF, Taus RH, Ganz P, Friedman PL, Levin DC. Side branch occlusion complicating percutaneous transluminal coronary angioplasty. *Radiology.* 1986;161:681-3.

6. Furukawa E, Hibi K, Kosuge M, Nakatogawa T, Toda N, Takamura T, Tsukahara K, Okuda J, Ootsuka F, Tahara Y, Sugano T, Endo T, Kimura K, Umemura S. Intravascular ultrasound predictors of side branch occlusion in bifurcation lesions after percutaneous coronary intervention. *Circ J.* 2005;69:325-30.

7. Achenbach S, Moselewski F, Ropers D, Ferencik M, Hoffmann U, MacNeill B, Pohle K, Baum U, Anders K, Jang IK, Daniel WG, Brady TJ. Detection of calcified and noncalcified coronary atherosclerotic plaque by contrast-enhanced, submillimeter multidetector spiral computed tomography: a segment-based comparison with intravascular ultrasound. *Circulation*. 2004;109:14-7.

8. Leber AW, Becker A, Knez A, von Ziegler F, Sirol M, Nikolaou K, Ohnesorge B, Fayad ZA, Becker CR, Reiser M, Steinbeck G, Boekstegers P. Accuracy of 64-slice computed tomography to classify and quantify plaque volumes in the proximal coronary system: a comparative study using intravascular ultrasound. *J Am Coll Cardiol.* 2006;47:672-7.

9. Hildick-Smith D, Lassen JF, Albiero R, Lefevre T, Darremont O, Pan M, Ferenc M, Stankovic G, Louvard Y. Consensus from the 5th European Bifurcation Club meeting. *EuroIntervention.* 2010;6:34-8.

10. Stankovic G, Darremont O, Ferenc M, Hildick-Smith D, Louvard Y, Albiero R, Pan M, Lassen JF, Lefèvre T; European Bifurcation Club. Percutaneous coronary intervention for bifurcation lesions: 2008 consensus document from the fourth meeting of the European Bifurcation Club. *EuroIntervention.* 2009;5:39-49.

11. Austen WG, Edwards JE, Frye RL, Gensini GG, Gott VL, Griffith LS, McGoon DC, Murphy ML, Roe BB. A reporting system on patients evaluated for coronary artery disease. Report of the Ad Hoc Committee for Grading of Coronary Artery Disease, Council on Cardiovascular Surgery, American Heart Association. *Circulation.* 1975;51:5-40.

12. Medina A, Suarez de Lezo J. Percutaneous coronary intervention in bifurcation lesions. Does classification aid treatment selection? *Rev Esp Cardiol.* 2009;62:595-8.

13. Kunita E, Fujii T, Urabe Y, Tsujiyama S, Maeda K, Tasaki N, Sekiguchi Y. Coronary plaque stabilization followed by color code plaque analysis with 64-slice multidetector row computed tomography. *Circ J.* 2009;73:772-5.

14. Uetani T, Amano T, Kunimura A, Kumagai S, Ando H, Yokoi K, Yoshida T, Kato B, Kato M, Marui N, Nanki M, Matsubara T, Ishii H, Izawa H, Murohara T. The association between plaque characterization by CT angiography and post-procedural myocardial infarction in patients with elective stent implantation. *JACC Cardiovasc Imaging.* 2010;3:19-28.

15. van der Giessen AG, Wentzel JJ, Meijboom WB, Mollet NR, van der Steen AF, van de Vosse FN, de Feyter PJ, Gijsen FJ. Plaque and shear stress distribution in human coronary bifurcations: a multislice computed tomography study. *EuroIntervention.* 2009;4:654-61.

16. Steigen TK, Maeng M, Wiseth R, Erglis A, Kumsars I, Narbute I, Gunnes P, Mannsverk J, Meyerdierks O, Rotevatn S, Niemela M, Kervinen K, Jensen JS, Galloe A, Nikus K, Vikman S, Ravkilde J, James S, Aaroe J, Ylitalo A, Helqvist S, Sjogren I, Thayssen P, Virtanen K, Puhakka M, Airaksinen J, Lassen JF, Thuesen L. Randomized study on simple versus complex stenting of coronary artery bifurcation lesions: The Nordic bifurcation study. *Circulation.* 2006;114:1955-61.

17. Ferenc M, Gick M, Kienzle RP, Bestehorn HP, Werner KD, Comberg T, Kuebler P, Buttner HJ, Neumann FJ. Randomized trial on routine vs. provisional T-stenting in the treatment of de novo coronary bifurcation lesions. *Eur Heart J.* 2008;29:2859-67.

18. Latib A, Colombo A. Bifurcation disease: What do we know, what should we do? *JACC Cardiovasc Interv.* 2008;1:218-26.

19. Hildick-Smith D, de Belder AJ, Cooter N, Curzen NP, Clayton TC, Oldroyd KG, Bennett L, Holmberg S, Cotton JM, Glennon PE, Thomas MR, Maccarthy PA, Baumbach A, Mulvihill NT, Henderson RA, Redwood SR, Starkey IR, Stables RH. Randomized trial of simple versus complex drug-eluting stenting for bifurcation lesions: the British Bifurcation Coronary Study: old, new, and evolving strategies.*Circulation.* 2010;121:1235-43.

20. Colombo A, Bramucci E, Sacca S, Violini R, Lettieri C, Zanini R, Sheiban I, Paloscia L, Grube E, Schofer J, Bolognese L, Orlandi M, Niccoli G, Latib A, Airoldi F. Randomized study of the crush technique versus provisional side-branch stenting in true coronary bifurcations: the CACTUS (Coronary Bifurcations: Application of the Crushing Technique Using Sirolimus-Eluting Stents) Study. *Circulation.* 2009;119:71-8.

21. Biondi-Zoccai GG, Lotrionte M, Moretti C, Meliga E, Agostoni P, Valgimigli M, Migliorini A, Antoniucci D, Carrie D, Sangiorgi G, Chieffo A, Colombo A, Price MJ, Teirstein PS, Christiansen EH, Abbate A, Testa L, Gunn JP, Burzotta F, Laudito A, Trevi GP, Sheiban I. A collaborative systematic review and meta-analysis on 1278 patients undergoing percutaneous drug-eluting stenting for unprotected left main coronary artery disease. *Am Heart J.* 2008;155:274-83.

22. Meliga E, Garcia-Garcia HM, Valgimigli M, Chieffo A, Biondi-Zoccai G, Maree AO, Cook S, Reardon L, Moretti C, De Servi S, Palacios IF, Windecker S, Colombo A, van Domburg R, Sheiban I, Serruys PW ; DELFT (Drug Eluting stent for LeFT main) Registry. Longest available clinical outcomes after drug-eluting stent implantation for unprotected left main coronary artery disease: the DELFT (Drug Eluting stent for LeFT main) Registry. *J Am Coll Cardiol*. 2008;51:2212-9.

23. Tamburino C, Angiolillo DJ, Capranzano P, Di Salvo M, Ussia G, La Manna A, Guzman LA, Galassi AR, Bass TA. Long-term clinical outcomes after drug-eluting stent implantation in unprotected left main coronary artery disease. *Catheter Cardiovasc Interv.* 2009;73:291-8.

24. Valgimigli M, Malagutti P, Aoki J, Garcia-Garcia HM, Rodriguez Granillo GA, van Mieghem CA, Ligthart JM, Ong AT, Sianos G, Regar E, Van Domburg RT, De Feyter P, de Jaegere P, Serruys PW. Sirolimus-eluting versus paclitaxel-eluting stent implantation for the percutaneous treatment of left main coronary artery disease: a combined RESEARCH and T-SEARCH long-term analysis. *J Am Coll Cardiol*. 2006;47:507-14.

25. Medina A, Suarez de Lezo J, Pan M. [A new classification of coronary bifurcation lesions]. *Rev Esp Cardiol.* 2006;59:183.

26. Tamburino C, Capranzano P, Capodanno D, Tagliareni F, Biondi-Zoccai G, Sanfilippo A, Caggegi A, Barrano G, Monaco S, Tomasello SD, La Manna A, Di Salvo M, Sheiban I. Plaque distribution patterns in distal left main coronary artery to predict outcomes after stent implantation. *JACC Cardiovasc Interv.* 2010;3:624-31.

27. Abizaid AS, Mintz GS, Abizaid A, Mehran R, Lansky AJ, Pichard AD, Satler LF, Wu H, Kent KM, Leon MB. One-year follow-up after intravascular ultrasound assessment of moderate left main coronary artery disease in patients with ambiguous angiograms. *J Am Coll Cardiol.* 1999;34:707-15.

28. Hermiller JB, Buller CE, Tenaglia AN, Kisslo KB, Phillips HR, Bashore TM, Stack RS, Davidson CJ. Unrecognized left main coronary artery disease in patients undergoing interventional procedures. *Am J Cardiol*. 1993;71:173-6.

29. Hu FB, Tamai H, Kosuga K, Kyo E, Hata T, Okada M, Nakamura T, Fujita S, Tsuji T, Takeda S, Motohara S, Uehata H. Intravascular ultrasound-guided directional coronary atherectomy for unprotected left main coronary stenoses with distal bifurcation involvement. *Am J Cardiol.* 2003;92:936-40.

30. Leesar MA, Masden R, Jasti V. Physiological and intravascular ultrasound assessment of an ambiguous left main coronary artery stenosis. *Catheter Cardiovasc Interv*. 2004;62:349-57.

31. Nakamura M, Nishikawa H, Mukai S, Setsuda M, Nakajima K, Tamada H, Suzuki H, Ohnishi T, Kakuta Y, Nakano T, Yeung AC.

Impact of coronary artery remodeling on clinical presentation of coronary artery disease: an intravascular ultrasound study. *J Am Coll Cardiol*. 2001;37:63-9.

32. Yamagishi M, Hosokawa H, Saito S, Kanemitsu S, Chino M, Koyanagi S, Urasawa K, Ito K, Yo S, Honye J, Nakamura M, Matsumoto T, Kitabatake A, Takekoshi N, Yamaguchi T. Coronary disease morphology and distribution determined by quantitative angiography and intravascular ultrasound--re-evaluation in a cooperative multicenter intravascular ultrasound study (COMIUS). *Circ J*. 2002;66:735-40.

33. Oviedo C, Maehara A, Mintz GS, Araki H, Choi SY, Tsujita K, Kubo T, Doi H, Templin B, Lansky AJ, Dangas G, Leon MB, Mehran R, Tahk SJ, Stone GW, Ochiai M, Moses JW. Intravascular ultrasound classification of plaque distribution in left main coronary artery bifurcations: Where is the plaque really located? *Circ Cardiovasc Interv.* 2010;3:105-12.

34. Medina A, Martin P, Suarez de Lezo J, Novoa J, Melian F, Hernandez E, Pan M, Burgos L, Amador C, Morera O, Garcia A. Ultrasound study of the prevalence of plaque at the carina in lesions that affect the coronary bifurcation. Implications for treatment with provisional stent. *Rev Esp Cardiol.* 2011;64:43-50.

35. Cunningham KS, Gotlieb AI. The role of shear stress in the pathogenesis of atherosclerosis. *Lab Invest.* 2005;85:9-23.

36. Malek AM, Alper SL, Izumo S. Hemodynamic shear stress and its role in atherosclerosis. *JAMA.* 1999;282:2035-42.

37. Vassilev D, Gil RJ. Relative dependence of diameters of branches in coronary bifurcations after stent implantation in main vessel--importance of carina position. *Kardiol Pol.* 2008;66:371-8; discussion 379.

38. Vassilev D, Gil R. Clinical verification of a theory for predicting side branch stenosis after main vessel stenting in coronary bifurcation lesions. *J Interv Cardiol*. 2008;21:493-503.

39. Kawasaki T, Koga H, Serikawa T, Orita Y, Ikeda S, Mito T, Gotou Y, Shintani Y, Tanaka A, Tanaka H, Fukuyama T, Koga N. The bifurcation study using 64 multislice computed tomography. *Catheter Cardiovasc Interv.* 2009;73:653-8.

40. Pflederer T, Ludwig J, Ropers D, Daniel WG, Achenbach S. Measurement of coronary artery bifurcation angles by multidetector computed tomography. *Invest Radiol.* 2006;41:793-8.

41. Finet G, Gilard M, Perrenot B, Rioufol G, Motreff P, Gavit L, Prost R. Fractal geometry of arterial coronary bifurcations: a quantitative coronary angiography and intravascular ultrasound analysis. *EuroIntervention.* 2008;3:490-8.

42. Murray CD. The physiological principle of minimum work: I. The vascular system and the cost of blood volume. *Proc Natl Acad Sci U S A.* 1926;12:207-14.